Ionization and excitation probabilities of a hydrogen atom suddenly released from penetrable confinement

Milagros F. Morcillo, José M. Alcaraz-Pelegrina and Antonio Sarsa

Departamento de Física, Campus de Rabanales Edif. C2, Universidad de Córdoba, E-14071 Córdoba, Spain

ARTICLE HISTORY
Compiled November 2, 2018

ABSTRACT
The problem of the stability of the hydrogen atom when it is released from a confining environment is studied. The stability is analysed in terms of excitation and ionization probabilities of the final state for different initial states. A spherical confining cavity of finite barrier height v_0 with inner radius r_0 and thickness Δ with the nuclear position at its center has been considered. The ionization probability presents different sharply peaked, non-symmetric local maxima as a function of the confinement size. This behaviour is related to the energy of the initial confined state that presents several maxima and minima in a kink-like structure as a function of the confinement size. The physical origin of these effects has been explained in terms of tunnelling and re-tunnelling of the atomic states. The sudden approximation and the analytic continuation method have been employed.

KEYWORDS
Confined atoms; ionization probability; sudden approximation

1. Introduction

It is well known that the energy levels of a confined system are different from those of the free system, hence its physical and chemical properties such as the atomic size, electronic structure, laser induced transition and excitation probabilities or chemical reactivity are modified when the atom is confined, see e.g. Refs. [1–10]. This has motivated a lot of interest in these systems for applications in different areas. For example the use of nanostructures as atomic and molecular containers [11–14], which could be very convenient for the storage and transport of hydrogen for its use as a clean source of energy [15], or in Medicine to get better radiopharmaceuticals [16, 17]. Other interesting applications would be the fabrication of semiconductors as quantum dots [18], or in optoelectronics with atomic levels tuned to provide specific emission features [19], and for the separation and diffusion of molecules through nanopores of low-dimensional carbon materials [20] or hydrogen and deuterium for its use as energy sources [21, 22].

In view of these kind of applications one may pose the question of the stability of the encapsulated species when they are suddenly released from confinement. For a possible use as nanocontainers, the encapsulated species should remain stable when

CONTACT A. Sarsa. Email: fa1sarua@uco.es

they are removed from confinement. The stability should not be taken from granted because the energy levels of the confined species are different from those of a free atom or molecule. A physical picture is to consider that the cavity exerts pressure on the confined atom, and this pressure disappears when the atom leaves the nanocapsule. This change on the atomic conditions gives rise to instabilities (the final state without confinement is not stationary) that may lead to ionization or dissociation in the case of molecules. Although the change of properties of confined atoms and molecules have been widely studied in the literature, see e.g. Ref. [23] for an extensive compilation of results, less information is available in the literature on the stability of the atomic or molecular species when confinement is removed [24].

Here we tackle the problem of the stability of an atom when it is extracted from a penetrable confining environment. Stability is characterized here as the ionization probability of a confined atom when it is released from confinement. We study a simple confinement situation that contains relevant physical aspects of the problem. We consider a confined hydrogen atom which, despite its simplicity, it can help to understand how other more complex systems behave under confinement. A spherical confining cavity of finite barrier height v_0 with inner radius r_0 and thickness Δ with the nuclear position at its center has been considered. This is a model of penetrable confining environments [25–28] which will introduce new effects not described by impenetrable walls [24]. In this work we shall study the s states of the hydrogen atom. We focus on the effects of the confinement size on the stability of the final states when the atom is released. We assume that the time needed to eliminate confinement can be neglected. Under this approximation one can obtain numerically exact solutions that will allow us to understand the time evolution of the atom when it is released. These solutions can be employed as a starting point for more elaborate descriptions of the extraction of confined species. Atomic units are used through out this work.

2. Methodology

We consider a hydrogen atom confined by a finite spherical barrier, $v_c(r)$,

$$H^{\rm c} = H + v_c(r), \tag{1}$$

where H is the Hamiltonian of the free hydrogen atom

$$H = -\frac{1}{2}\nabla^2 - \frac{Z}{r}, \tag{2}$$

with Z the nuclear charge and $v_c(r)$ the confining potential

$$v_c(r) = \begin{cases} v_0 & \text{if} \quad r_0 \leq r \leq r_0 + \Delta \\ 0 & \text{otherwise,} \end{cases} \tag{3}$$

where, r_0, is the inner radius, v_0, the height and, Δ, the width of the barrier.

We assume that the confined atom is in a stationary state, $\Psi^{\rm c}_{nlm}$

$$H^{\rm c}\ \Psi^{\rm c}_{nlm}(\vec{r}) = E^{\rm c}_{nl}\, \Psi^{\rm c}_{nlm}(\vec{r}). \tag{4}$$

Due to the spherical symmetry of the confinement barrier, the confined state can be

written as

$$\Psi^{\rm c}_{nlm}(\vec{r}) = \frac{u^{\rm c}_{nl}(r)}{r} Y_{lm}(\Omega). \tag{5}$$

As in our previous work [24], the analytic continuation method [29–31] has been used to obtain all the radial functions involved in the calculation. The radial Schrödinger equation is written as

$$\frac{d^2 u_l}{dr^2} + \left[2E + \frac{2Z}{r} - \frac{l(l+1)}{r^2}\right] u = 0 \tag{6}$$

An uniform grid in the radial coordinate is employed. A polynomial expansion of the radial function in each interval is carried out

$$u(r) = \begin{cases} r^{l+1} \sum_{i=0}^{N} a_i r^i & 0 \le r \le r_1 \\ \sum_{i=0}^{N} c_{ki} (r - r_k)^i & r_k \le r \le r_{k+1}, \quad k = 1, 2, \ldots \end{cases} \tag{7}$$

The coefficients a_i and c_{ki} are calculated by using a three term recursion relationship obtained by substituting Eq. 7 into the radial Schrödinger equation, Eq. 6. The values of the radial function and its first derivative at r_{k+1}, $k = 0, 1 \ldots$, needed to build the solution around that point, are obtained from the series at the previous tabular point, while at $r_0 = 0$, the regularity and normalization conditions are used. A step size of 10^{-3} and a value of $N = 20$ has been employed. Bound state energies are calculated carrying out inward and outward integrations and imposing continuity of the logarithmic derivative at an intermediate point.

The ionization probability, P_I, is calculated as

$$P_{\rm I} = \int_0^\infty dE \, |C^{nl}(E)|^2, \tag{8}$$

where $|C^{nl}(E)|^2 \, dE$ represents the probability that the electron, initially in the $\Psi^{\rm c}_{nlm}$ confined state, becomes ionized with energy between E and $E + dE$ when confinement is removed. Within the sudden approximation here employed, the $C^{nl}(E)$ distribution functions are obtained as

$$C^{nl}(E) = \int_0^\infty dr \, u^{\rm f}_{El}(r) u^{\rm c}_{nl}(r), \tag{9}$$

where $u^{\rm f}_{El}(r)$ is the reduced radial function of the ionized hydrogen atom with energy E and orbital angular momentum l, normalized in the energy scale

$$\int_0^\infty dr \, u^{\rm f}_{El}(r) u^{\rm f}_{E'l}(r) = \delta(E - E'). \tag{10}$$

The ionization probability can also be obtained in terms of P_B, the probability that the atom remains in a bound state when confinement is removed, as

$$P_{\rm I} = 1 - P_{\rm B}, \tag{11}$$

where

$$P_{\rm B} = \sum_{n'=1}^{\infty} |C_{n'}^{nl}|^2, \tag{12}$$

and

$$C_{n'}^{nl} = \int_0^{\infty} dr\, u_{n'l}^{\rm f}(r) u_{nl}^{\rm c}(r). \tag{13}$$

Finally, it is worth mentioning here the energy of the initial confined state, $E_{nl}^{\rm c}$, is not equal to the energy of the final unconfined state, $E^{\rm f}$, evaluated as the expectation value of the unconfined Hamiltonian in the final state. The relation between these two energy values is

$$E_{nl}^{\rm c} = E^{\rm f} + \int d\vec{r}\; \Psi_{nlm}^{\rm c}(\vec{r})^*\, v_c(r) \Psi_{nlm}^{\rm c}(\vec{r}). \tag{14}$$

3. Results and discussion

Here we have employed fixed values of the potential height, $v_0 = 2.5$ and width, $\Delta = 5$, as in [27]. Energies and ionization probabilities are studied as a function of the confinement size r_0.

In Figure 1, we plot the energy of the confined $3s$-$6s$ states as a function of the confinement size r_0. The energy of each orbital is negative in the whole range and presents local maxima and minima at different r_0 values. This function is neither smooth at the maxima nor at the minima. The position of the maxima of one orbital energy coincides with the position of the minima of the following orbital, with very similar energy values. The number of maxima is equal to the principal quantum number of the orbitals. As it could be expected, those orbitals with a larger spatial extension are affected by confinement at larger distances. Both, the oscillatory behaviour of the orbital energy with the sawtooth structure shown in Figure 1, and the fact that the energy is always negative, were not obtained for an infinite barrier [24]. This is because for a finite barrier the orbital may extend over the entire space while for the infinite barrier the orbital is confined between the nucleus and the barrier.

Figure 1

We focus on the $4s$ orbital first which is representative for the rest of cases. For a barrier size of $r_0 = 70$, the orbital is practically unaffected by confinement. As one considers smaller confinement sizes, the energy of the orbital increases. This is because the state shrinks and the electronic charge becomes more localized in space. A kink is found at $r_0 = 26.2$, corresponding to a local maximum of the energy for this confinement size. For the same r_0 value, a local minimum, also with a kink structure, is found for the $5s$ orbital energy. The two energy values are very similar, $E_{4s} = -0.01821$ and $E_{5s} = -0.01820$.

In order to elucidate the physical origin of these kinks in the energy we start by analysing the $4s$ orbital. In Figure 2, we plot the reduced radial function of the $4s$ state for $r_0 = 27$ and $r_0 = 26$, i.e. before and after the kink. The unconfined reduced radial orbital is also shown for the sake of comparison. For $r_0 > 26.2$ we have the usual trend: the orbital is within the confinement region and smaller confinement sizes give

rise to orbitals less extended in space with larger energies. For a confinement size of $r_0 = 26$ the state has tunnelled out and the charge density is beyond the barrier. The radial function is practically negligible inside the confinement region and it looks like a ground state wave function outside the barrier, i.e. it is nodeless for $r \geq r_0 + \Delta$. The nodes of the $4s$ reduced radial orbital for $r_0 = 26$ are not visible in the scale of the figure. This sudden enhancement of confined orbitals by penetrable barriers was also obtained in Ref. [27] for the $1s$, $2s$ and $2p$ states of the hydrogen atom for r_0 between 1.45 and 1.59 and for some semifilled shell atoms [28].

Figure 2

As the confinement size is reduced from 26 to 15, the $4s$ orbital lies mostly outside the wall and its energy decreases as r_0 decreases within this range. The $3s$ orbital is inside the confinement region and, as the confining size decreases, the orbital is compressed to the nucleus and its energy increases. At $r_0 = 14.52$, both orbitals present very similar energies, $E_{3s} = -0.02664$ and $E_{4s} = -0.02663$. For r_0 values below 14.52 an abrupt change in the slopes is found in such a way that for the $4s$ the energy increases as r_0 decreases and the opposite holds for the $3s$. This is due to the tunnelling of both orbitals as it is shown in Figure 3, where we plot the radial functions of the confined $3s$ (upper panel) and $4s$ (lower panel) orbitals for $r_0 = 14$, 15 and 26. For $r_0 = 15$ the $3s$ orbital behaves like a second excited state within the confinement region (two nodes) while for $r_0 = 14$ it looks like a ground state outside the barrier (nodeless in that region) The nodes are imperceptible within the scale of the figure. The opposite holds for the $4s$ orbital, which enters into the confinement area for $r_0 < 14.52$ and behaves like a second excited state there with two visible nodes inside the confinement volume (the third node cannot be distinguished within the scale of the figure). As r_0 further decreases from 14, the energy of the $4s$ increases because the orbital contracts into the inner region while the $3s$, outside the barrier, becomes more bound. This gives rise to the opposing sawtooth structure with facing peaks shown in Figure 1.

Figure 3

This pattern of tunnelling and re-tunnelling processes is repeated for all states for different r_0 values. As r_0 decreases the separation between the maxima and minima becomes narrower and more orbital pairs become involved in a smaller r_0 range. This is illustrated in Figure 4, where we plot the reduced radial function of the $1s$ to $5s$ orbitals for $r_0 = 5.9,\ 6.0$ and 6.1 in the upper, medium and lower panels respectively. The potential is also shown in the figures with arbitrary units in the y axes. For $r_0 = 5.9$ one can find in the inner region the $1s$ state with zero nodes and the $5s$ with one visible node. These states present a typical ground and first excited state structure in this region and are negligible outside the confinement region. The $2s$, $3s$ and $4s$ orbitals present the typical ground and excited states behaviour outside the wall with zero, one and two nodes beyond the barrier. The other nodes of these orbitals cannot be distinguished within the scale employed. These orbitals are practically negligible inside the confinement region. For $r_0 = 6.0$ the scheme is the same with a change of roles between the $4s$ and $5s$ orbitals, the former has tunnelled in while the later has tunnelled out. Finally, for $r_0 = 6.1$ the change of roles is between the $3s$ and $4s$ states. This behaviour has an effect on the energy of the orbitals that presents a sawtooth structure. Within this r_0 range the $1s$ orbital is inside while the $2s$ orbital is outside the confinement region. The energy of the $3s$ has a peak at $r_0 = 6.1$ that is a minimum, and another peak at $r_0 = 6.0$ that is a maximum. The peak at $r_0 = 6.0$ of 4s orbital is a minimum and the maximum is located at $r_0 = 5.9$, the same position where one minimum of the $5s$ orbital energy is located.

Figure 4

In general, as the barrier approaches the nucleus from the unconfined situation, and the charge becomes compressed through the nucleus, the orbital energy increases. At a given r_0 value, a ns orbital tunnels through the barrier to the outermost region and the $(n+1)s$ orbital, that was outside, comes into the confinement area. The first time this ns orbital tunnels out, it will be nodeless in the outermost region. As r_0 further decreases, the ns state will tunnel back in and the $(n-1)s$ will tunnel out. The first time the ns orbital tunnels back inside the confinement region it will have $n-2$ nodes in that region. When the charge density is inside the barrier, the energy increases as r_0 decreases and the opposite holds when the charge density is outside. The change on the slope is given by tunnelling, which takes place for a particular r_0 value, giving rise to kinks in the energy as a function of r_0. For successive tunnellings the number of nodes outside the confinement region will increase by one and the number of nodes inside will decrease by one. This gives a limitation on the number of tunnellings of a given orbital and therefore in the number of maxima and minima of the energy versus r_0. As it should be the case, the global energy ordering the orbitals depends on the total number of nodes distributed according to Sturm's theorem.

The abrupt changes on the electronic charge distributions for different confinement sizes will have an impact on the ionization probability, P_I. In Figure 5 we plot the ionization probability of the different states here studied as a function of the inner radius of the barrier. In the inset, we show the ionization probability only for the $4s$, $5s$ and $6s$ orbitals for r_0 between 20 and 32. For r_0 values different from those where tunnelling takes place, the ionization probability shows an oscillatory behaviour, as it was the case of the infinite barrier [24]. A significant rise in the ionization probability of the $4s$ state is observed as r_0 is reduced from $r_0 = 35$ to $r_0 = 26.2$. For these values the orbital lies inside the confinement region. The tunnelling of the $4s$ orbital gives rise to a steep drop of the ionization probability. The $5s$ orbital tunnels in at this r_0 value causing an abrupt rise in its ionization probability. The ionization probability of this orbital is further increased as r_0 is diminished and it drops abruptly when the $5s$ orbital tunnels out again at $r_0 = 24.39$, where the $6s$ tunnels in and its ionization probability increases. This scheme is repeated as successive orbitals tunnel inside and outside the barrier for different confinement sizes. Thus, when the charge density is outside the cage, the electron is more likely to remain bound when confinement is removed, and when it is inside the cage, the ionization probability increases. If one characterizes the stability of a confined state as the probability of not being ionized when confinement is removed, we find that some more stable initial states can be obtained by reducing the size of the confining box. In the neighbourhood of the critical radii where orbitals tunnel, the energies of the tunnelling orbitals are very similar but the charge distribution is very different. Thus, the ionization probability of these two near degenerate orbitals is very different. Therefore, for these confining barriers the energy of the initial confined states is not an indication of the stability after confinement removal.

Figure 5

When the ionization probability drops sharply for a given initial state, the probability that the atom remains in a excited bound state increases, see Eq. 11. For an initial $4s$ confined orbital, we plot in Figure 6 the transition probabilities to each possible final unconfined bound state, $P_{4s\to ns}$. Results for confining sizes of $r_0 = 26$ and $r_0 = 27$ are shown. The general trend is similar, but there quantitative differences are found. For $r_0 = 27$ the final unconfined state with the largest probability is the $4s$, while for $r_0 = 26$ is the $5s$ with a substantially higher value of the probability.

Figure 6

In Figure 7, we plot in the upper panel the free $4s$ orbital and the confined $4s$ orbital for $r_0 = 27$. These two orbitals are similar within the confinement region which leads to an important overlap between them. In the lower panel of Figure 7 we plot the confined $4s$ orbital for $r_0 = 26$ and the free $5s$ orbital. For this confinement situation, the $4s$ orbital has tunnelled out and the charge distribution is negligible within the confinement region. Outside the barrier, this orbital is similar to the free $5s$ orbital. The overlap with the free $4s$ is strongly hindered while the overlap with the free $5s$ is increased, giving rise to a higher probability for the later.

Figure 7

The effect of the barrier height and width has been investigated by carrying out calculations for different v_0 and Δ values. The same qualitative behaviour of the ionization probability of the states shown in Figure 5 is obtained for v_0 values between 1 and 20 and Δ values between 1 and 10. For fixed Δ, as v_0 increases the position of the peaks is shifted to larger r_0 values. For example, for $\Delta = 5$, the local maximum of the ionization probability of the $3s$ orbital located at $r_0 = 6.04$ for $v_0 = 2.5$, is at $r_0 = 5.85$ for $v_0 = 1$ and at $r_0 = 6.30$ for $v_0 = 10$. The height of the peaks increases as v_0 does. Thus the value of this local maximum is 0.24 for $v_0 = 1$, 0.27 for $v_0 = 2.5$ and 0.28 for $v_0 = 10$. At fixed v_0, lower values of Δ leads to lower peaks shifted towards larger r_0 values. For example, the local maximum of the $3s$ orbital located at $r_0 = 6.04$ for $v_0 = 2.5$ and $\Delta = 5$, is shifted to $r_0 = 6.17$ and $r_0 = 6.30$ for $\Delta = 2$ and $\Delta = 1$ respectively for the same v_0. The height is reduced from 0.27 for $\Delta = 5$ to 0.26 and 0.21 for $\Delta = 2$ and $\Delta = 1$ respectively. Higher barriers lead to wider peaks of the ionization probability because the state tunnels out (reducing abruptly its ionization probability) at smaller r_0 values. Narrower barriers give rise to wider ionization probability peaks because for smaller Δ values the the state tunnels in at larger r_0 values. In both cases, the effect is not very significant in the range considered.

4. Conclusions

The stability of a hydrogen atom after leaving confinement is studied in terms of the ionization probability of its different confined levels. A model of penetrable spherical barrier is considered for the confinement. It has been assumed that the time needed to extract the atom is small. Only s states have been considered in this study. The ionization probability of a given state presents different sharply peaked, non-symmetric maxima as a function of r_0. This behaviour has been interpreted in terms of the tunnelling outside and inside the barrier of confined levels for different confinement sizes. This also leads to a sawtooth structure of the energy when it is plotted as a function of the confinement radius. When a state tunnels out through the barrier, another state tunnels inside the confinement region and both present very similar energies, but the balance between the kinetic energy and the potential energy is different when the orbital is inside or outside the barrier. The position of the nodes is modified in such a way that, the first time the ns orbital tunnels outside the confinement region it is nodeless in that domain. In successive tunnelings the number of nodes outside the barrier is increased by one while the opposite holds when the orbital tunnels back inside the confining region. This leads to a limitation of the number of tunnelings of a given orbital and therefore in the number of peaks of the ionization probability as a function of r_0. When the state leaves the confinement region, the ionization probability decreases abruptly and the probability that the atom is in a excited bound

state increases. The opposite holds when the orbitals tunnels back in the confinement region.

Acknowledgements

AS would like to thank Dra. M^{a} Pilar de Lara Castells for many fruitful discussions and encouraging conversations during the realization of this and other works.

Funding

This work was partially supported by the Spanish Dirección General de Investigación Científica y Técnica (DGICYT) and FEDER under contract FIS2015-69941-C2-2-P and the Junta de Andalucía under Grant FQM378. The work of MFM was partially supported by a PhD fellowship from Spanish Ministerio de Ciencia, Innovación y Universidades under Grant FPU16/05950. The work of AS was partially supported by the COST Action CM1405 MOLIM.

References

[1] J.C.A. Boeyens, Journal of the Chemical Society Faraday Transactions **90**, 3377 (1994).
[2] V.K. Dolmatov, A.S. Baltenkov, J.P. Connerade and S.T. Manson, Radiat. Phys. Chem. **70**, 417 (2004).
[3] D.M. Mitnik, J. Randazzo and G. Gasaneo, Physical Review A **78**, 062501 (2008).
[4] S.H. Patil and Y.P. Varshni, Adv. Quantum Chem. **57**, 1 (2009).
[5] J. Sabin, E. Brändas and S. Cruz, editors, *Theory of Confined Quantum Systems* (Elsevier, Oxford, UK, 2009).
[6] J.P. Connerade, Journal of Physics: Conference Series **438**, 012001 (2013).
[7] K.D. Sen, editor, *Electronic Structure of Quantum Confined Atoms and Molecules* (Springer-Verlag, Switzerland, 2014).
[8] S. Lumb, S. Lumb and V. Prasad, Phys. Rev. A **90**, 032505 (2014).
[9] R. Cabrera-Trujillo, R. Méndez-Fragoso and S.A. Cruz, Journal of Physics B: Atomic, Molecular and Optical Physics **49**, 015005 (2015).
[10] S. Lumb, S. Lumb and V. Prasad, Phys. Lett. A **379**, 1263 (2015).
[11] C. Liu, Y.Y. Fan, M. Liu, H.T. Cong, H.M. Cheng and M.S. Dresselhaus, Science **286**, 1127–1128 (1999).
[12] P. Moriarty, Reports on Progress in Physics **64**, 297–381 (2001).
[13] A.J. Horsewill, K.S. Panesar, S. Rols, M.R. Johnson, Y. Murata, K. Komatsu, S. Mamone, A. Danquigny, F. Cuda, S. Maltsev, M.C. Grossel, M. Carravetta and M.H. Levitt, Physical Review Letters **102**, 013001 (2009).
[14] A. Krachmalnicoff, R. Bounds, S. Mamone, S. Alom, M. Concistre, B. Meier, K. Kouril, M.E. Light, M.R. Johnson, S. Rols, A.J. Horsewill, A. Shugai, U. Nagel, T. Room, M. Carravetta, M.H. Levitt and R.J. Whitby, Nature Chemistry **8**, 953 (2016).
[15] K. Ayub, International Journal Of Hydrogen Energy **42**, 11439 (2017).
[16] D.W. Cagle, S.J. Kennel, S. Mirzadeh, J.M. Alford and L.J. Wilson, Proceedings of the National Academy of Sciences **96**, 5182–5187 (1999).
[17] T. Li and H.C. Dorn, Small **13**, 1603152 (2017).
[18] L. Jacak, O. Hawrylak and A. Wojs, *Quantum Dots* (Springer-Verlag, Berlin-Heidelberg, 1998).
[19] M. Anaya, A. Rubino, T.C. Rojas, J.F. Galisteo-López, M.E. Calvo and H. Míguez, Advanced Optical Materials **5**, 1601087 (2017).

[20] Y. Jiao, A. Du, M. Hankel and S.C. Smith, Physical Chemistry Chemical Physics **15**, 4832–4843 (2013).
[21] T.M. Nenoff, R.J. Spontak and C.M. Aberg, MRS Bulletin **31**, 735–744 (2006).
[22] M. Hankel, H. Zhang, T.X. Nguyen, S.K. Bhatia, S.K. Gray and S.C. Smith, Physical Chemistry Chemical Physics **13**, 7834 (2011).
[23] E. Ley-Koo, Rev. Mex. Fis. **64**, 326–363 (2018).
[24] M.F. Morcillo, J.M. Alcaraz-Pelegrina and A. Sarsa, International Journal of Quantum Chemistry **118**, e25563 (2018).
[25] J.P. Connerade, V.K. Dolmatov and P.A. Lakshmi, Journal of Physics B: Atomic, Molecular and Optical Physics **33**, 251–264 (2000).
[26] J.P. Connerade, V.K. Dolmatov and S.T. Manson, Journal of Physics B: Atomic, Molecular and Optical Physics **33**, 275–282 (2000).
[27] V.K. Dolmatov and J.L. King, Journal of Physics B: Atomic, Molecular and Optical Physics **45**, 225003–1–225003–5 (2012).
[28] V.K. Dolmatov, Journal of Physics B: Atomic, Molecular and Optical Physics **46**, 095005–1–095005–6 (2013).
[29] A. Holubec and A.D. Stauffer, Journal of Physics A: Mathematical and Theoretical **18**, 2141 (1985).
[30] R.J.W. Hodgson, Journal of Physics A: Mathematical and Theoretical **21**, 679 (1988).
[31] E. Buendía, F.J. Gálvez and A. Puertas, Journal of Physics A: Mathematical and Theoretical **28**, 6731 (1995).

Figures

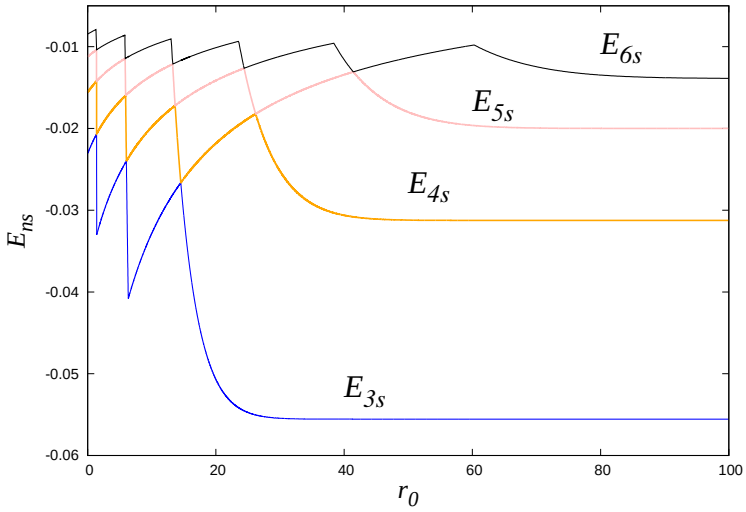

Figure 1. M.F. Morcillo, J.M. Alcaraz-Pelegrina, A. Sarsa.

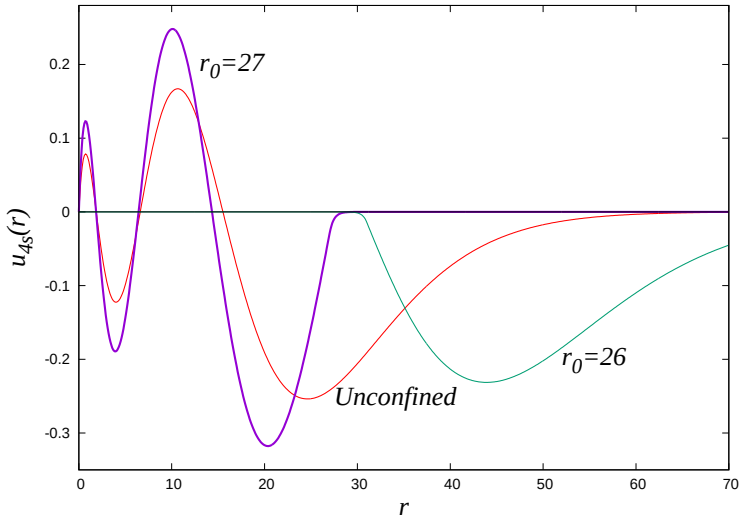

Figure 2. M.F. Morcillo, J.M. Alcaraz-Pelegrina, A. Sarsa.

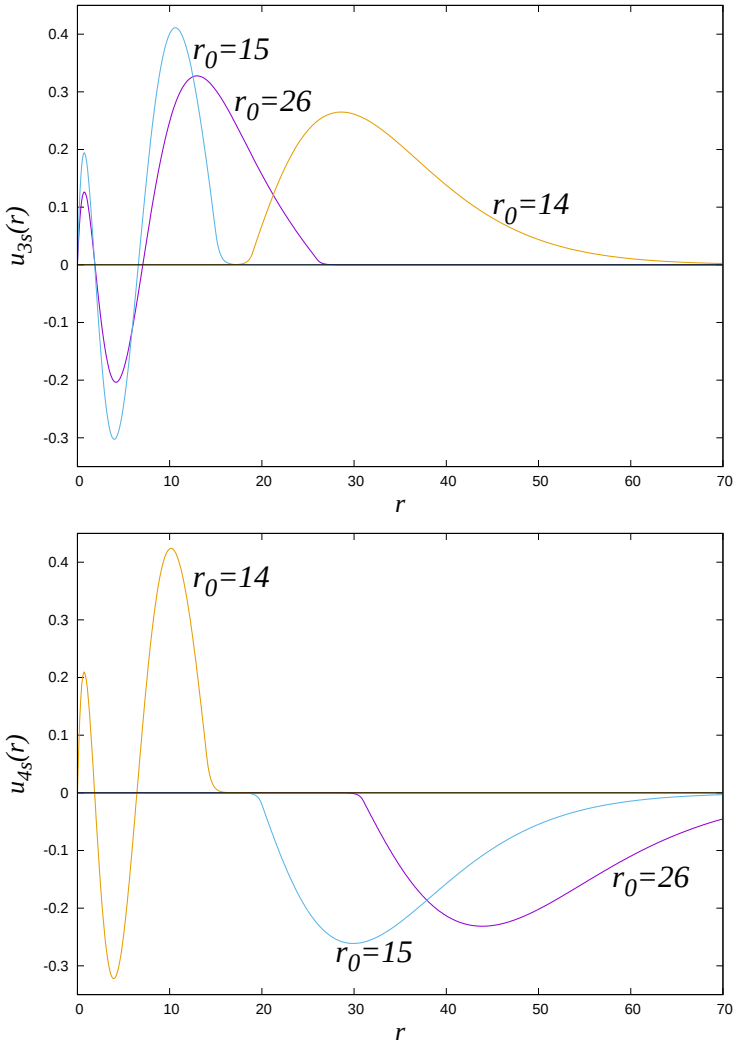

Figure 3. M.F. Morcillo, J.M. Alcaraz-Pelegrina, A. Sarsa.

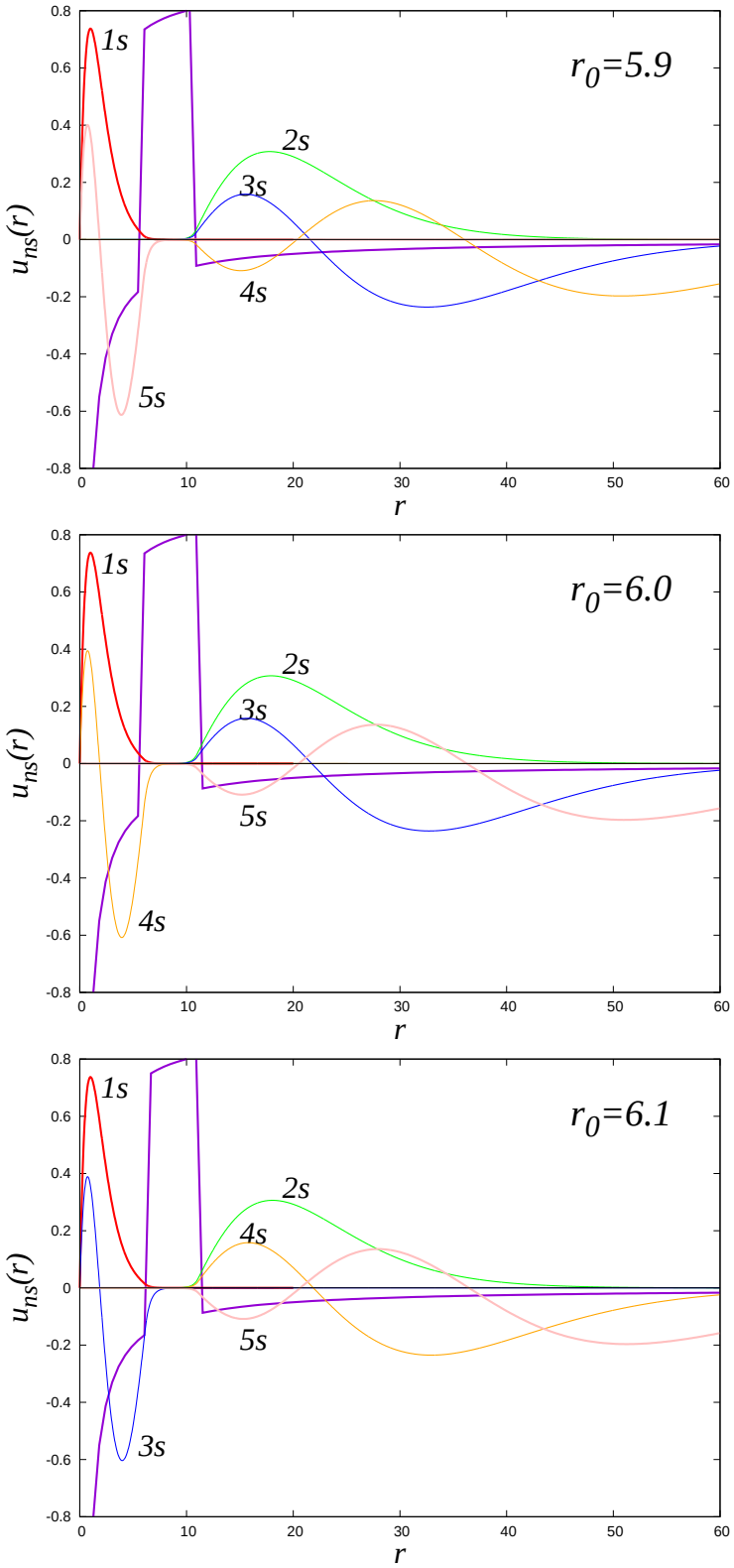

Figure 4. M.F. Morcillo, J.M. Alcaraz-Pelegrina, A. Sarsa.

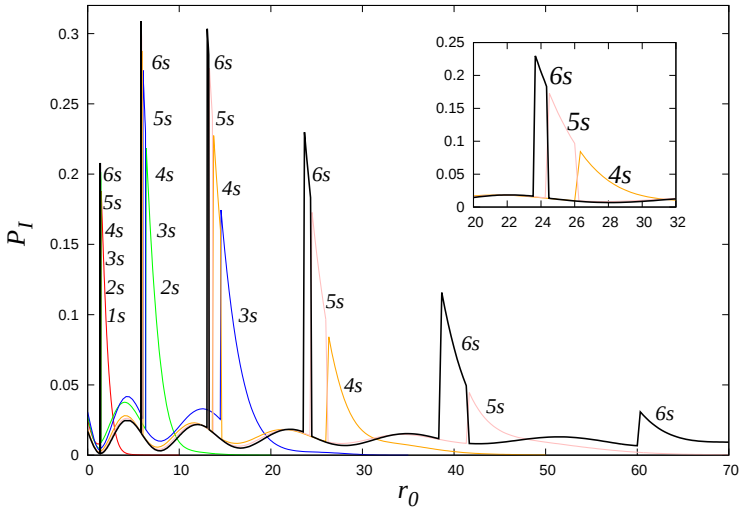

Figure 5. M.F. Morcillo, J.M. Alcaraz-Pelegrina, A. Sarsa.

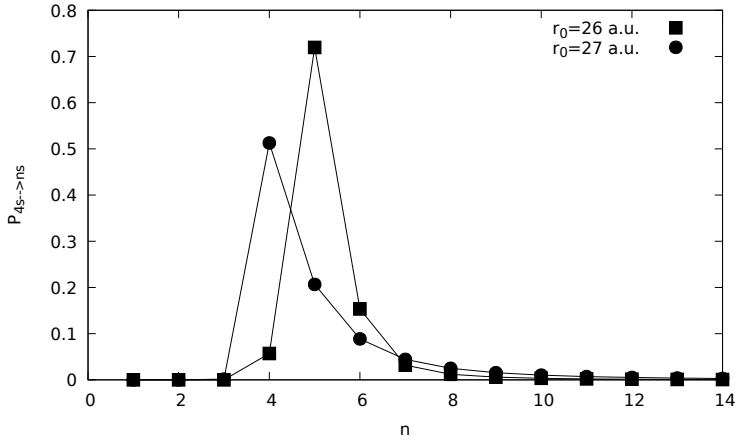

Figure 6. M.F. Morcillo, J.M. Alcaraz-Pelegrina, A. Sarsa.

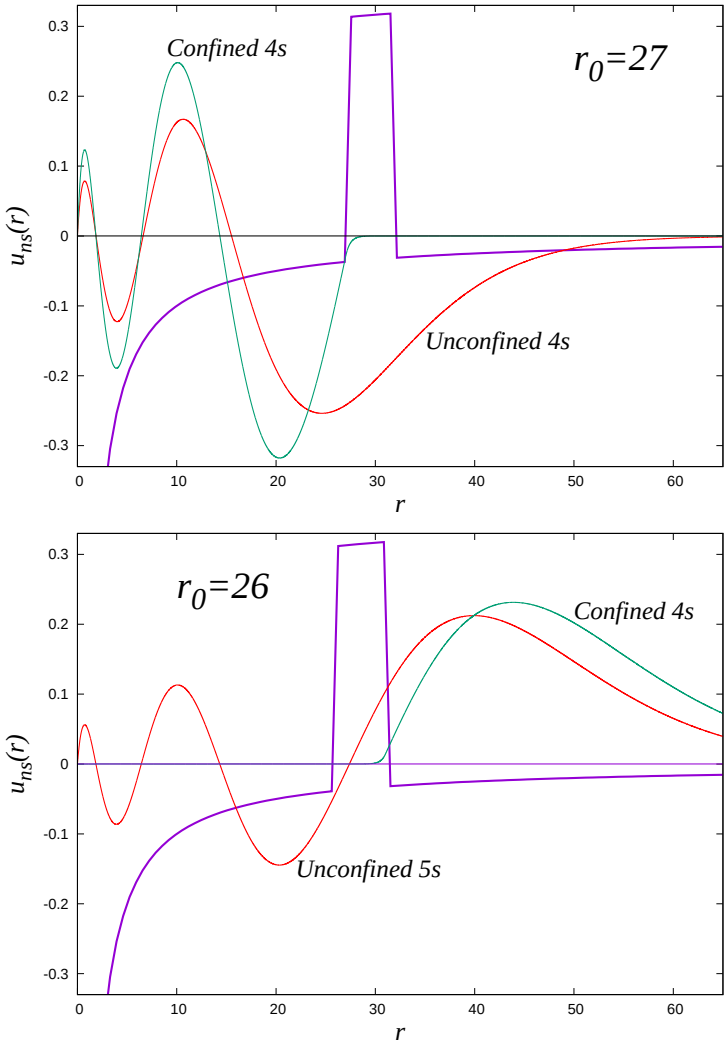

Figure 7. M.F. Morcillo, J.M. Alcaraz-Pelegrina, A. Sarsa.

Figure captions

Figure 1. Energy of the confined $3s$ to $6s$ states as a function of the confinement size, r_0.

Figure 2. Reduced radial functions, $u(r)$, of the confined $4s$ for confinement sizes of $r_0 = 26$ and $r_0 = 27$. The radial orbital of the unconfined atom is also shown.

Figure 3. Upper panel: For the $3s$ orbital, reduced radial functions, $u(r)$, for $r_0 = 26$, 15 and 14. Lower panel: The same for the $4s$ orbital.

Figure 4. Upper panel: Reduced radial functions, $u(r)$, of the $1s$ to $5s$ orbitals for a confinement size of $r_0 = 5.9$. The potential is also shown in arbitrary units in the y axes. Medium panel: The same orbitals for $r_0 = 6.0$. Lower panel: The same orbitals for $r_0 = 6.1$.

Figure 5. Ionization probability of the $1s$-$6s$ states as a function of r_0. In the inset the ionization probability in a reduced r_0 range is shown for the $4s$, $5s$ and $6s$ orbitals.

Figure 6. Transition probability to bound s states of the unconfined atom for an inital $4s$ confined state for confinement sizes of $r_0 = 26$ and $r_0 = 27$. The solid lines are for guiding the eye.

Figure 7. Upper panel: Reduced radial function, $u(r)$, for a confined $4s$ orbital for $r_0 = 27$ as compared with the free $4s$ orbital. The potential in arbitrary units in the y axes is also plotted. Lower panel: Reduced radial function, $u(r)$, for a confined $4s$ orbital for $r_0 = 26$ as compared with the free $5s$ orbital. The potential in arbitrary units in the y axes is also ploted.